[AMERICAN JOURNAL OF SCIENCE, VOL. 279, DECEMBER, 1979, P. 1089-1107]

American Journal of Science

DECEMBER 1979

THE STRUCTURE AND EMPLACEMENT OF CINDER CONE FIELDS

MARK SETTLE

Department of Geological Sciences,
Brown University,
Providence, Rhode Island 02912

ABSTRACT. Terrestrial cinder cone fields generally occur in two types of volcanic provinces, either: (1) upon the flanks of major volcanoes, or (2) within relatively flat-lying volanic fields. Measurements of cone shape and distribution have been performed in three volcano cone fields (Mauna Kea, Hawaii; Mt. Etna, Italy; Kilimanjaro, Tanzania) and three platform cone fields (San Francisco Mtn., Ariz.; Paricutin region, Mexico; Nunivak Island, Alaska). Modal average values of cone basal diameter are on the order of 300 to 400 m within volcano cone fields and 900 to 1000 m within platform cone fields. Cone height/diameter ratios are generally smaller within the platform cone fields. Variations in cone shape cannot be directly attributed to different eruption conditions, however, since cone morphometry is also a function of weathering environment and exposure age. Modal average values of cone separation distance range from 600 to 800 m within volcano cone fields to 1000 to 1200 m within platform cone fields. Comparison of average morphometric parameters for the six fields indicates that cone diameter is positively correlated with cone separation distance. Furthermore, the size (diameter) and spacing of cinder cones formed on the flanks of volcanoes is generally less than the size and spacing of cones constructed in volcanic fields. Historical observations indicate that flank eruptions commonly shift to higher or lower elevations in response to variations in magmatic pressure. Such shifts would tend to limit the growth of individual cones and would also result in smaller separation distances between cones. Comparable variations in vent location are less likely to occur within volcanic fields due to smaller regional topographic differences and the general lack of regional rift zones.

INTRODUCTION

Terrestrial cinder cone fields occur in two distinctive types of volcanic provinces. Cinder cones are commonly found on the flanks of major volcanoes such as Mauna Kea (Hawaii) and Kilimanjaro (Tanzania). Cinder cones also occur in relatively flat-lying volcanic terranes in association with extensive lava flow deposits as observed in the San Francisco Mtn. volcanic field (Arizona) and the Nunivak Island volcanic field (Alaska). The former type of occurrence will be referred to here as *volcano cone fields*, and the latter type of occurrence will be termed *platform cone fields*. The term "platform" generally denotes a planar, raised surface. However, it is used here in a more restricted sense to refer to a regional surface that may be slightly warped or inclined but is relatively flat and level in comparison to the exterior flanks of a major volcano.

Conical structures resembling terrestrial cinder cones have been identified on the Moon and Mars (McGetchin and Head, 1973; Head, 1975; Carr and others, 1977). The morphology of these landforms can

potentially provide valuable information about explosive volcanic processes operating on other planetary surfaces. In order to make meaningful comparisons between eruption conditions on the Earth and other planetary bodies, it is first necessary to determine the natural morphological variability of terrestrial cones and to evaluate the influence of erosive processes upon cone shapes.

The spatial distribution and alignment of cinder cones can also provide information about crustal structure and regional fracture systems. Regional correlations between cone distribution patterns and fracture patterns in specific cinder cone fields have been noted by field investigators. However, the physical factors governing the emplacement of cinder cone fields in different types of volcanic provinces have not been generally determined. The spatial distribution of cones on other planetary surfaces could be used to investigate crustal structure, if terrestrial magma migration processes were better understood.

This paper reports the results of a comparative geomorphological study of six terrestrial cinder cone fields. The purposes of this study are: (1) to characterize statistically the structure of terrestrial cinder cones, (2) to determine if cone shape or spacing is uniquely correlated with the type of volcanic province in which a cone field occurs, and (3) to explore the volcanic processes responsible for the construction of cinder cone fields.

DATA COLLECTION AND PRESENTATION

Morphometric measurements were performed in three volcano cone fields (Mauna Kea, Mt. Etna, and Kilimanjaro) and three platform cone fields (San Francisco field, Ariz.; Paricutin region in Mexico; and the Nunivak Island field, Alaska). The location, age, and current weathering environment of each field is documented in table 1. The position, basal diameter, and, if possible, the height of each cinder cone within an individual field were determined using the map products cited in table 1. High resolution topographic maps of the Paricutin region and Kilimanjaro were not immediately available for this study. Consequently, cinder cone heights were not determined in these two fields. Measurements of cone location and diameter were performed upon an electronic digitizing board (accuracy ± 0.01 inch).

Cinder cones consist principally of interbedded deposits of fragmental, pyroclastic material produced by moderately explosive eruptions. Intrusive dikes and sills and interbedded lava flows typically constitute a small fraction of a cone's total volume (Atwood, 1906; Gutmann, 1976). In many cases spatter cones may have the same general appearance as cinder cones; however, spatter cones are principally composed of agglutinated lava globules which are generally produced by weakly explosive eruptions. In practice, it can be quite difficult to determine the relative proportions of cinder and spatter within an individual cone, particularly if field exposures of interior cone structure are limited. For the purposes of this study cinder cones were identified on

TABLE 1

Summary of cone field location, age, and current weathering environment for the six fields examined in this study

Cinder cone field	Age of cones	Current Weathering Environment		Reconnaissance geology references	Map products
		Climatic conditions	Annual precipitation (Reporting Station)		
Mauna Kea (19.8°N, 155.4°W)	Majority of cones <0.3m.y.	Tropical - Subarctic	355.6 cm (Hilo, Hawaii)	Stearns and Macdonald (1946) Macdonald (1949) Porter (1972)	U.S. Geol. Survey topographic maps 7.5 min series (scale 1:24000, 40 ft contour interval)
Mt. Etna (37.7°N, 15°E)	All cones - <0.3m.y.	Temperate - Subarctic	90.8 cm (Catania, Sicily)	Rittmann (1963, 1973) Huntington and others (1974)	Italian Military Geographic Institute topographic maps (scale 1 cm = 250 m, 25 m contour interval)
Kilimanjaro (3°S, 37.3°E)	Majority of cones <0.5m.y.	Semi-arid - Tropical - Subarctic	85.9 cm (Moshi)	Downie and Wilkinson (1972)	Geological map of Kilimanjaro by Downie and Wilkinson (scale 1:125000, 500 ft contour interval)
San Francisco Mtn. (35.4°N, 111.7°W)	Majority of cones <1m.y.	Semi-arid	46.5 cm (Flagstaff, Arizona)	Robinson (1913) Colton (1967) Moore and Wolfe (1976) Moore, Wolfe, Ulrich (1976)	U.S. Geol. Survey topographic maps 7.5 min series (scale 1:24000, 20 ft contour interval), 15 min series (scale 1:62500, 40 ft contour interval)
Paricutin Region (19.5°N, 102.1°W)	Majority of cones <0.1 m.y.	Tropical - Temperate	168.3 cm (Uruapan)	Williams (1950)	Geological reconnaissance map of Paricutin region by Williams and Peria, plate 8. U.S. Geol. Survey Bull. 965 (scale 1" ≈3.1 km)
Nunivak Island (60°N, 166.3°W)	Majority of cones <0.3m.y.	Arctic	38.6 cm (Nunivak, Alaska)	Hoare and others (1968) D. Francis, unpub. field notes	U.S. Geol. Survey topographic maps 1:63300 series (50 ft contour interval)

Previous reconnaissance studies and relevant map products are cited. Annual precipitation data are given for weather stations situated in or near each cone field (after Wernstedt, 1972). Precipitation measurements at a single reporting station may not accurately represent the amount of annual precipitation received throughout each cone field, particularly in the case of volcano cone fields.

the basis of geological reconnaissance maps prepared by earlier field investigators (see references in table 1). The criteria used to classify cinder cones are not explicitly described in these regional mapping studies.

The absolute number of cinder cones identified within a particular cone field may differ somewhat from estimates provided by previous studies (see table 2). Certain cones were either too small or too degraded to be clearly distinguished on available topographic maps. Only those cones that could be positively identified with reference to specific reconnaissance maps were included in this study. Some cinder cones may have been overlooked by field investigators, whereas other cone-like features such as large scale spatter cones may have been mapped erroneously as cinder cones by reconnaissance surveys. However, the large number of cones observed in each field ensures that average morphometric parameters determined in this study are truly representative of cinder cone structure and distribution within specific cone fields.

Cone basal diameter is reported here as the average (mean) of the maximum and minimum base diameters measured for each cone. The location of a cone's basal edge was determined in one of two ways, either: (1) explicitly from published reconnaissance maps (this procedure was followed for the Paricutin and Kilimanjaro cones), or (2) by direct measurement of the point of topographic inflection along a cone's exterior surface (this inflection point is defined by an abrupt change in the spacing and/or circularity of topographic contours outlining a cone). Cone height is reported here as the difference between the average basal elevation and the maximum elevation observed at the cone's rim crest or summit. Cone separation distance is reported here as the horizontal distance between a cinder cone and its nearest neighbor and was mea-

TABLE 2

Percentile values determined from frequency distributions of various morphometric parameters measured within individual cinder fields

Cinder cone field	Number of cones	Cone basal diameter (m)	Cone height (m)	Cone separation distance (m)
		25th/50th/75th percentile	25th/50th/75th percentile	25th/50th/75th percentile
Mauna Kea	168	396/ 508/ 650	47/ 67/100	569 / 813/1524
Mt. Etna	87	311/ 369/ 471	36/ 57/ 87	425 / 780/1373
Kilimanjaro	205	477/ 673/ 951	—	679 /1152/1879
San Francisco Mtn.	376	889/1158/1497	80/111/166	989 /1367/1971
Paricutin Region	170	615/ 848/1000	—	831 /1149/1783
Nunivak Island	83	661/ 850/1284	34/ 53/ 72	1047/1547/2955

The fiftieth percentile represents the median value of a parameter frequency distribution. Fifty percent of the data points contained in each parameter frequency distribution lie between the twenty-fifth and seventy-fifth percentile values. (Note cinder cone height was not determined within the Kilimanjaro and Paricutin cone fields.)

sured between the centers of two cones. Cinder cone clusters in which the pyroclastic aprons of two or more cones are contiguous or overlapping exist in all of the cone fields examined. Cluster members have been considered as individual cones in instances in which separate eruptive vents could be distinguished.

Frequency distributions of cone parameters generally correspond to Poisson distributions rather than Gaussian (normal) distributions. Due to the inherent asymmetry of Poisson distributions, *median* values of cone dimensions are considered to characterize the average morphometry of a particular cinder cone field more accurately than the arithmetric mean value of each distribution. Median values of cone basal diameter, cone height, and cone separation distance for each cinder cone field are reported in table 2.

CINDER CONE FIELDS: GENERAL STRUCTURE AND CHARACTERISTICS

Platform cone fields.—The San Francisco Mtn. volcanic field was constructed by three major cycles of volcanic activity separated by periods of broad crustal uplift and faulting that altogether spanned a period of at least 6 m.y. (Robinson, 1913; Moore, Wolfe, and Ulrich, 1976). The current eruption cycle has produced ~80 km^3 of basaltic lava flows and ~200 cinder cones (Robinson, 1913). This eruptive cycle was preceded by a period of more silicic eruptions (lavas ranging from andesites to rhyolites) and a still earlier period of basaltic fissure eruptions (Robinson, 1913). Cinder cones have been emplaced throughout Quaternary and late Pliocene time; volcanic activity has migrated eastward during this period. Approximately half the cones included in the data set formed during the last million years (Moore, Wolfe, and Ulrich, 1976; Colton, 1967). The San Francisco cone field extends over an area of 6100 km^2 and an elevation range of 1080 m. In an overall sense, cinder cones are widely scattered throughout the field; however, local groups of cones are commonly aligned subparallel to regional fracture systems. For example, groupings of 30 to 80 cones appear to be preferentially aligned along common azimuthal directions extending 20 to 40 km north and east of San Francisco Mtn. Areal cone density averaged over the entire field is 6.3 cones/100 km^2. Maximum cone density of ~3.2 cones/10 km^2 occurs within a 150 km^2 area surrounding Sunset Crater.

Nunivak Island is situated within the Bering Sea about 40 km from the Alaskan coastline. The island was constructed over the past 6 m.y. by a series of extrusive eruptions that alternately produced alkalic and tholeiitic basalts (Hoare and others, 1968). The majority of cinder cones found on Nunivak Island formed over the past 0.3 m.y. during a period of alkalic basalt eruption that produced ~2.3 km^3 of lava and pyroclastics. This eruptive phase was preceded by a period of tholeiite basalt eruption (0.9-0.3 m.y. before present) that produced ~130 km^3 of lava (Hoare and others, 1968). Cinder cones are distributed over an area of ~3000 km^2 and an elevation range of 305 m.

In general, cones are widely scattered within an east-west trending belt (fig. 1). However, subgroupings of cones appear to be locally aligned along common azimuthal directions extending over distances of 5 to 10 km. Areal cone density averaged over the entire field is 2.8 cones/100 km^2. Maximum cone density of 1.8 cones/10 km^2 occurs within a 110 km^2 area north and west of Mt. Roberts.

The Paricutin cone field examined in this study is a small section of the Mexican Volcanic Belt in the immediate vicinity of the Paricutin volcano. The current phase of volcanic activity in this region has produced flows and pyroclastic material consisting of olivine basalts and olivine-bearing basaltic andesites. This eruption cycle was preceded by a period of andesitic eruption (Williams, 1950). Cinder cones have

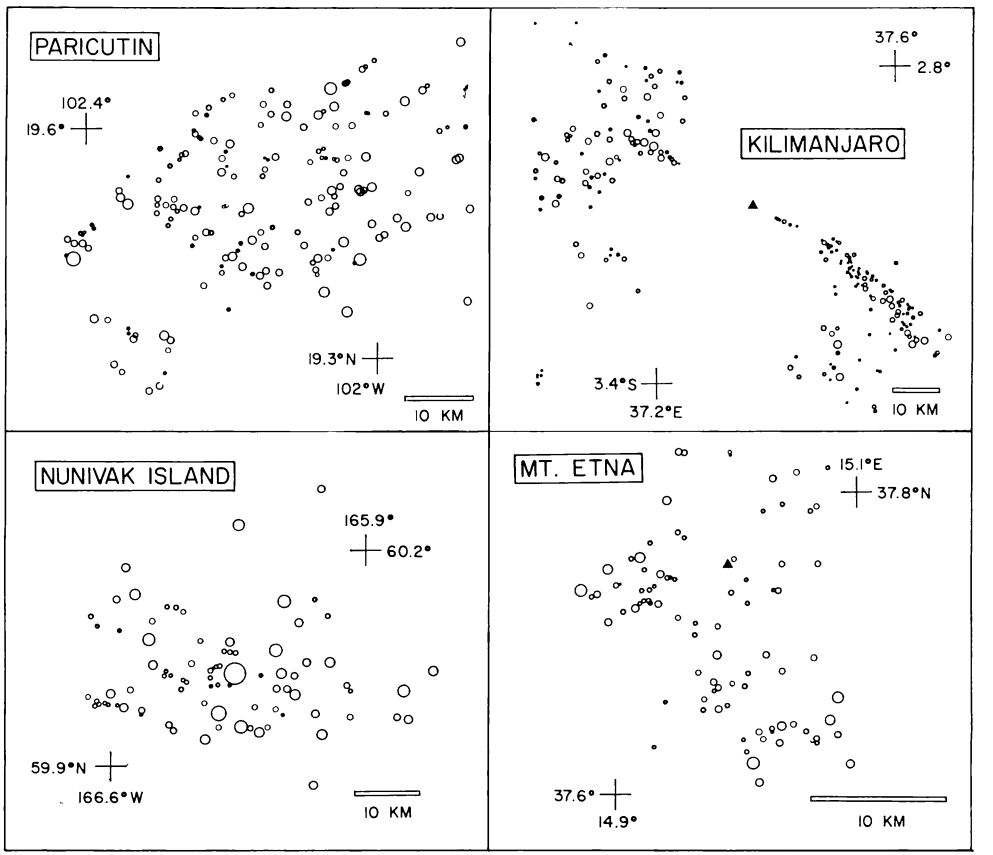

Fig. 1. Plan view of cinder cone distribution patterns at Kilimanjaro and Mt. Etna (volcano cone fields) and at Paricutin and Nunivak Island (platform cone fields). Individual cinder cones are represented by circles with diameters proportional to the cone's average basal diameter (see scale bar in each diagram). Volcano summits are indicated by solid triangles in the case of Kilimanjaro and Mt. Etna. Note that cinder cones occurring within volcanic fields are widely scattered; whereas cones formed on the flanks of volcanoes are generally clustered in radial sectors emanating from the volcano's summit.

been constructed throughout Quaternary time, though most of the cones included in the data set probably formed during the last 0.1 m.y. (Williams, 1950). The Paricutin cone field extends over an area of 2300 km^2 and a range of elevation amounting to several hundred meters. Williams observed that "within the Paricutin region most of the cones appear to be scattered haphazardly" (Williams, 1950, p. 189; see fig. 1). Areal cone density averaged over the entire field is 7.5 cones/100 km^2. Maximum cone density of ~1.9 cones/10 km^2 was measured within a 90 km^2 area north and east of the town of San Lorenzo.

Volcano cone fields.—The Mauna Kea cone field on the island of Hawaii was emplaced during a period of alkalic basalt eruption. This eruptive phase was preceded by a period of tholeiite basalt eruption responsible for the construction of the basal shield that forms the foundation of the Mauna Kea edifice (Macdonald and Katsura, 1964). The majority of cinder cones found on the flanks of the Mauna Kea formed during the last 0.3 m.y. (Porter, Stuiver, and Yang, 1977; Macdonald, 1949; McDougall, 1964). Cones are distributed over an area of 1500 km^2 and an elevation range of 3580 m extending from near sealevel to the volcano's summit at ~4080 m. Cones have been constructed on all sides of the volcano; however, the majority of cones are concentrated within three zones radiating to the northeast, south-southeast, and west of the summit that extend over distances of 10 to 15 km. Gravity and magnetic surveys indicate that these radial zones are the surface expressions of major radial fractures that extend into the Mauna Kea edifice to varying depths (Malahoff and Woollard, 1966; Kinoshita, 1965). Areal cone density averaged over the entire field is 11.1 cones/100 km^2. Maximum cone density equal to 4.7 cones/10 km^2 was measured within a 74 km^2 rectangular area encompassing the south-southeast rift zone of the volcano.

The Mt. Etna volcanic edifice on the island of Sicily was constructed over the past 0.3 m.y. Therefore the cinder cone field situated on the flanks of this volcano must have been emplaced over some fraction of this time period. Detailed analysis of the chemical evolution of Etnean lavas and pyroclastics is currently in progress (Huntingdon and others, 1974). Cinder cones are distributed over an area of ~800 km^2 and an elevation range of 2675 m extending from near sealevel to the volcano's summit at ~3150 m. Although the Mt. Etna cones are not concentrated within well defined linear zones, they do appear to be preferentially clustered into certain general areas (see fig. 1). Cones occur in profusion on the south-southeast and western flanks of the volcano and are scarce or absent in areas to the north, east, and southwest of the volcano's summit (Tanguy and Kieffer, 1977; Wadge, 1978). Areal cone density averaged over the entire field is 11.3 cones/100 km^2. Maximum areal density of 3.9 cones/10 km^2 occurs within an 80 km^2 area on the south-southeast flank of the volcano.

Kilimanjaro is a massive volcano with three separate summit vents that have each served as major extrusive centers. The oldest cinder

cones on the flanks of Kilimanjaro were formed in early Quaternary time; however, the majority of cones included within the data set were constructed during late Pleistocene time (probably over the past 0.5 m.y.; see Downie and Wilkinson, 1972). The chemical relationships between the pyroclastic material produced by cone-forming eruptions and the alkalic basalt produced during earlier, shield-building phases of activity are not well understood (Downie and Wilkinson, 1972). Cones are distributed over an area of ~5400 km^2 and an elevation range of 3765 m extending from the base of the volcano at ~730 m to an elevation of 4500 m (summit elevation = 5800 m). Cinder cones are concentrated in two linear zones radiating northwest and southeast of the summit. These zones extend over distances of 15 to 40 km, respectively (see fig. 1). Cones are not observed directly north or south of the volcano's summit. Areal cone density averaged over the entire field is 3.8 cones/100 km^2. Maximum areal density of 4.0 cones/10 km^2 was measured within a 190 km^2 rectangular area enclosing the southeastern rift zone.

Discussion.—The six cinder cone fields discussed above were constructed over a roughly contemporaneous period of time. The majority of cones examined in this study are inferred to be no more than 300,000 yrs old. The average areal density of cinder cones within these six fields ranges from 3 to 11 cones/100 km^2. However, maximum values of local cone density are consistently greater within the volcano cone fields (4-5 cones/10 km^2) in which cinder cones are preferentially aligned along major rift zones. Cones constructed on the flanks of volcanoes have been emplaced over an elevation range of 2500 to 4000 m, whereas cones formed within relatively flat-lying volcanic fields were emplaced over a 300 to 1100 m elevation range. The advent of cone-forming eruptions does not appear to signal a unique stage in the chemical evolution or morphological development of a volcanic province. For example, in the case of Mt. Etna and Nunivak Island the eruptive phase in which cinder cones are constructed represents one stage in the initial evolution of a province; whereas at San Francisco Mtn. and Paricutin, basaltic cinder cone eruptions occur after a period of regional erosion and a preceding cycle of andesitic and rhyolitic eruptions.

CINDER CONE SHAPE

Influencing factors.—Since cinder cones are primarily constructed by moderately explosive eruptions, pristine cone morphometry depends principally upon explosive eruption conditions (that is, pyroclastic size distribution, ejection velocity, and ejection angle). In cases in which extrusive activity plays a minor role in the growth of a cinder cone, its initial shape will be determined mainly by ballistic deposition of pyroclastic material and the radial migration of its exterior talus apron by mass wasting processes (McGetchin, Settle, and Chouet, 1974).

Erosive processes operating upon a cone field may vary significantly as the regional weathering environment changes over geological time scales. For example, weathering deposits on the flanks of Mauna Kea

and Kilimanjaro provide direct evidence of recent glacial erosion near the summits of these two volcanoes (Porter, Stuiver, and Yang, 1977; Downie and Wilkinson, 1972). Even during a particular geological epoch cinder cones formed along the flanks of volcanoes may be exposed to a variety of weathering environments ranging from tropical conditions near the base of the volcano to subarctic conditions near the volcano's summit (for example, Kilimanjaro). In addition, Scott and Trask (1971) have suggested that since the ratio of cone surface area to cone volume decreases with increasing cone diameter, fluvial processes may erode smaller cinder cones at relatively faster rates. The temporal and spatial variability of weathering conditions and the possibility that erosion rates may be related to cone size can account for the wide variety of cone degradation states observed in a cone field (Colton, 1967). Differences in the exposure ages of individual cones will also contribute to the observed variability in cone morphometry.

Direct comparisons of the average dimensions of cinder cones occurring in two or more cone fields may reveal significant differences in cone shape that can be attributed to: (1) the nature of explosive volcanic activity forming the fields, and/or (2) the nature and duration of erosive processes operating upon the fields. Although one of these two factors may be principally responsible for observed differences in average cone morphometry, it is difficult to identify unambiguously the cause of such morphometric disparities due to limited knowledge of: (1) the variability of cone-forming eruptions, (2) the morphometric response of cinder cones to various erosive processes, and (3) the complete record of weathering conditions within individual cone fields.

Observations.—Relative frequency distributions of various morphometric parameters are presented in figure 2 for each cinder cone field. A relative frequency distribution is constructed by normalizing a parameter frequency distribution to the total number of cinder cones found within a particular field. In this manner the data for each field are equally weighted, even though the absolute number of cones within the individual fields varies by a factor of four. In figure 2 relative parameter frequency distributions determined for individual cone fields have been combined on the basis of the type of volcanic province in which the cone field formed. The data assembled in figure 2 should describe general morphometric differences between volcano cone fields and platform cone fields, provided that the six fields selected for analysis are representative examples of each cone field type.

A comparison of the combined frequency distributions of core basal diameter (D_{co}) indicates that the average diameter of cones constructed within volcanic fields is greater than the average diameter of cones formed on the flanks of volcanoes. Modal averages obtained from the combined distribution range from $D_{co} = 300$ to 400 m for volcano cone fields to $D_{co} = 900$ to 1000 m for platform cone fields (fig. 2A). Median values of D_{co} measured with individual cone fields range from 369 m at Mt. Etna to 1158 m at San Francisco Mtn. (table 2). Median

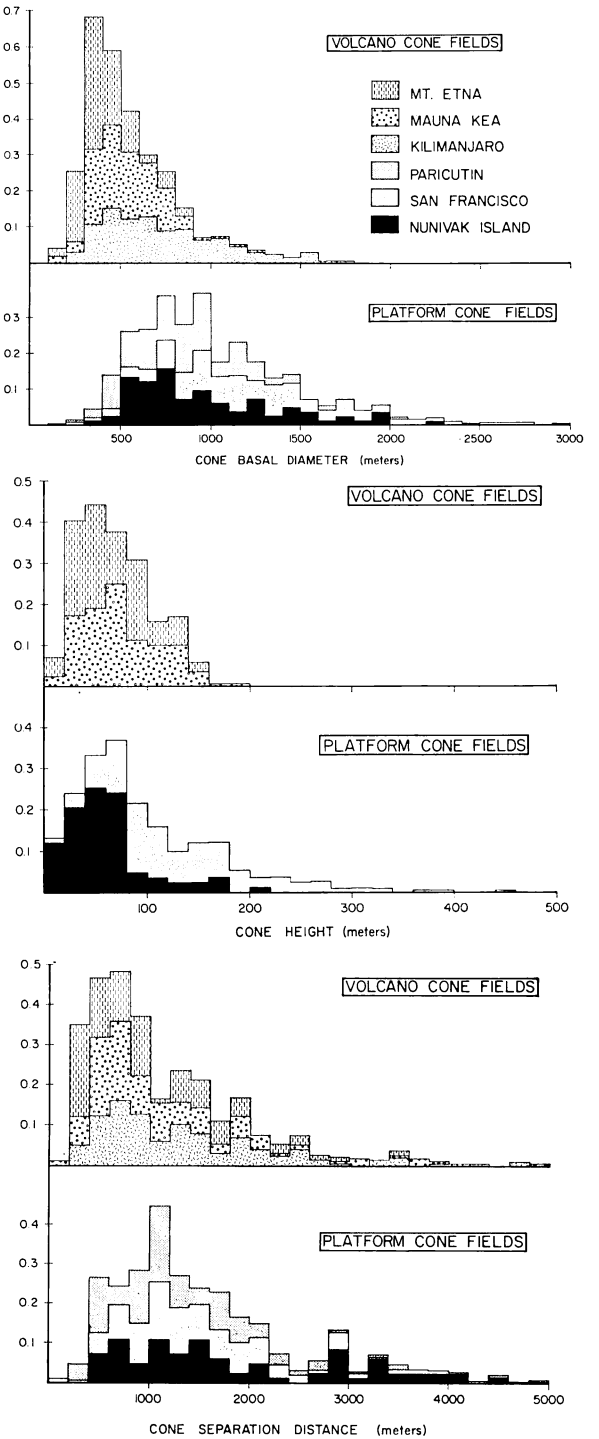

Fig. 2. Combined relative frequency distributions of (A) cone basal diameter, (B) cone height, and (C) cone separation distance. Relative frequency distributions of each parameter have been determined within individual cinder cone fields and are combined in these histograms on the basis of the type of volcanic province in which the cone field formed. The shaded areas representing individual cone fields within each of the combined parameter distributions are equal, so that data from each cone field are equally weighted in all three parameter distributions.

values of cone diameter associated with platform cone fields are consistently greater than median values of D_{co} determined for volcano cone fields (table 2).

No such systematic relationship was discovered between cone height (H) and field type. Median values of H determined within individual cone fields range from 53 m at Nunivak Island to 111 m at San Francisco Mtn. (table 2). Each of these cone fields occurs within a volcanic field, indicating that average cone height is not correlated with the type of volcanic province in which a cone field is constructed. Comparison of the combined cone height frequency distributions (fig. 2B) indicates that the average height of cinder cones within the two types of provinces is not markedly different. Modal averages obtained from the combined distributions range from H = 40 to 60 m for volcano cone fields and H = 60 to 80 m for platform cone fields. The cone height frequency distributions for Nunivak Island and San Francisco Mtn. are rather dissimilar, however, and the modal value of H determined from the combined distributions may not be generally representative of average cone height within platform cone fields.

Discussion.—Cone height (H) is plotted versus cone basal diameter (D_{co}) in figure 3. Porter (1972) has previously reported an empirical relationship between cone height and diameter in which $H = 0.18\ D_{co}$ based upon a select group of 30 Mauna Kea cinder cones presumably characterized by a fresh morphological appearance. Bloomfield (1975) has examined the morphometry of 41 cinder cones within a section of the Mexican Volcanic Belt to the east of Paricutin. He reported a mean cone height/diameter ratio for Holocene cones of 0.21 and a mean ratio of H/D_{co} of 0.19 for relatively young "well-formed" Pleistocene cones. Therefore the $H = 0.2\ D_{co}$ reference line shown in figure 3 may characterize the initial shape of cinder cones formed in both types of volcanic provinces prior to erosive degradation.

The majority of cinder cones at Mauna Kea plot somewhat below the $H = 0.2\ D_{co}$ reference line. This may be a consequence of erosive processes which simultaneously reduce cone height and increase a cone's basal diameter. Mauna Kea cones that are situated below the reference line in figure 3 are generally characterized by H/D_{co} ratios ranging from 0.20 to 0.10 (65 percent of the cones fall within this range). Similarly, the majority of Mt. Etna cinder cones plot below the $H = 0.2\ D_{co}$ reference line, although the shape of cones with rim heights greater than 70 m is reasonably well represented by the reference line (see fig. 3). At both Mauna Kea and Mt. Etna an appreciable number of cones are characterized by H/D_{co} ratios greater than 0.2 (12 percent of the Mauna Kea cones and 18 percent of the Mt. Etna cones fall in this category).

In contrast, the $H = 0.2\ D_{co}$ relationship appears to be an upper bound on distributions of H/D_{co} for cinder cones formed within the

two volcanic fields presented in figure 3. Half the cinder cones at San Francisco Mtn. are characterized by ratios of H/D_{co} less than 0.10. However, H/D_{co} ratios for some of the freshest cones within the field, such as Sunset Crater ($H/D_{co} = 0.18$), SP Crater ($H/D_{co} = 0.21$), and Strawberry Crater ($H/D_{co} = 0.18$), are closely approximated by the $H = 0.2\ D_{co}$ relationship. All the cinder cones on Nunivak Island possess H/D_{co} ratios less than 0.15. Half the Nunivak cones are characterized by H/D_{co} ratios less than 0.06.

The San Francisco Mtn. cone field has been emplaced throughout the latter half of Quaternary time (covering approx 1 m.y.) in contrast to the Mauna Kea field which has been primarily constructed over the past 300,000 yrs. A greater variety of cone degradation states would logically be anticipated within the older San Francisco field which has been exposed to erosive weathering processes for a longer period of time. The data in figure 3 indicate that cinder cones within the San

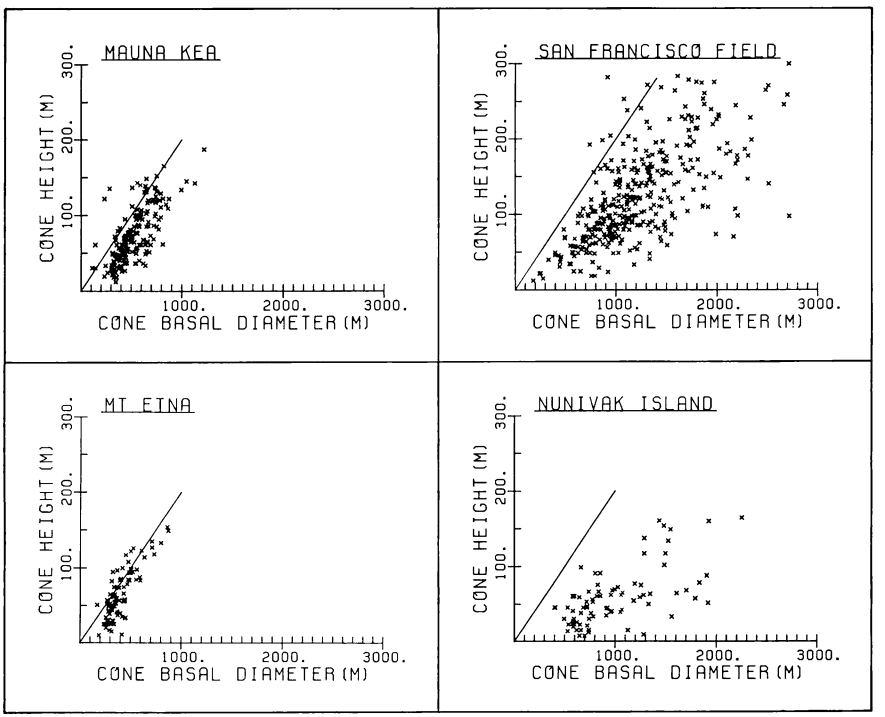

Fig. 3. Comparison of the shape of cinder cones found within four cone fields for which detailed topographic data were readily available. Cinder cone height, H (defined as the difference between a cone's basal elevation and the maximum elevation observed at the rim crest or summit of a cone), is graphed versus cone basal diameter, D_{co} (defined as the arithmetic mean of the maximum and minimum base diameter measured for each cone). The straight line in each graph represents the relationship $H = 0.2\ D_{co}$ which may describe the average initial shape of cinder cones prior to erosive degradation (see text for details).

Francisco field are significantly more degraded than those at Mauna Kea. Half the San Francisco cinder cones are characterized by $H/D_{co} < 0.1$, whereas only 23 percent of the Mauna Kea cones possess H/D_{co} ratios less than 0.10.

The Nunivak Island cone field, however, formed approximately contemporaneously with the Mauna Kea field and yet the Nunivak cones have much smaller H/D_{co} ratios than the Mauna Kea cones. These morphometric differences cannot be accounted for by variations between the exposure ages of the two cone fields. Rather, the observed differences in cone shape may result from the more severe weathering environment on Nunivak Island and/or differences between explosive eruption conditions in the two fields. Under current climatic conditions, permafrost exists over large portions of Nunivak Island (D. Francis, personal commun., 1978). Seasonal freeze-thaw cycles associated with permafrost may tend to accelerate the downslope movement of surficial material on the Nunivak cinder cones. Alternatively, cone-forming eruptions on Nunivak may have been somewhat more phreatic than typical cinder cone eruptions on Mauna Kea due to the presence of subsurface permafrost layers.

CINDER CONE DISTRIBUTION

Observations.—Relative frequency distributions of cone separation distance are presented in figure 2C. A comparision of the combined distributions indicates that the average spacing between cinder cones in volcanic fields is greater than average cone spacing on the flanks of volcanoes. Modal averages of cone separation distance (S_d) obtained from the combined frequency distributions are $S_d = 600$ to 800 m for volcano fields and $S_d = 1000$ to 1200 m for platform cone fields (fig. 2C). Median values of cone separation distance determined for individual cone fields range from 780 m at Mt. Etna to 1547 m at Nunivak Island (table 2). Although median values of cone spacing are generally greater within platform cone fields, median values of S_d determined at Kilimanjaro and Paricutin are not significantly different. Therefore cone spacing is not considered to be strictly correlated with the type of volcanic province in which a cone field occurs.

Discussion.—Volcanic field volcanism is generally initiated by a phase of regional extrusive activity consisting of widespread fissure eruptions that produce voluminous lava flow deposits (see Robinson, 1913; Hoare and others, 1968). The movement of magma accompanying this activity serves to create or activate multiple sets of regional fractures within the crustal layers underlying a volcanic field (Robinson, 1913; Williams, 1950; Bloomfield, 1975). In the course of subsequent explosive activity, magma may be funnelled into a variety of fracture intersections (accounting for the overall scattered distribution of cones observed within volanic fields), or it may be locally injected into regional fractures at depth (accounting for the local alignment of small groupings of cones observed within volcanic fields).

Major structural lineaments exposed along the flanks of volcanoes are interpreted to be the surface expressions of fracture zones that penetrate a volcano's edifice and commonly extend to the central magma conduit at the core of a volcano (Nakamura, 1977). These large scale fracture networks are commonly referred to as rift zones, and they are produced by: (1) the gravitational stresses acting upon a volcano, and (2) structural faults in basement materials (Fiske and Jackson, 1972). Rift zones represent paths of minimum mechanical resistance to fluid magma bodies. Tilt measurements at Kilauea (Hawaii) have shown that magma is frequently injected into rift zones to relieve magmatic pressure within the core of the volcano during or in-between summit eruptions (Eaton and Murata, 1960; Moore and Krivoy, 1964; Richter and others, 1970). Since these large-scale, continuous fracture zones provide such readily accessible avenues to the surface, it is not surprising that cinder cones are typically concentrated along the surface expressions of rift zones. However, a comparison of cone distribution patterns for Kilimanjaro and Mt. Etna (fig. 1) suggests that the actual degree of cone alignment exhibited by individual volcano cone fields can be quite variable and depends upon the interior configuration of radial and arcuate fractures penetrating a volcano's edifice (Wadge, 1978).

In summary, it would appear that cinder cone distribution patterns are, in effect, controlled by near-surface fracture systems. Within volcanic fields rising magma encounters multiple sets of crustal fractures and tends to be funnelled into fracture intersections to produce an overall scattered pattern of cone distribution. In contrast, magma rising within the central conduit of a volcano is more likely to be shunted into one of the major fracture zones within the volcano's edifice and discharged somewhere along the surface expression of the fracture. This generally produces a preferentially aligned pattern of cone distribution with individual cones concentrated in specific radial sectors on the flanks of the volcano. The cone spacing measurements reported in this study indicate that the widely scattered cinder cones found in volcanic fields are, on the average, separated by greater horizontal distances than preferentially aligned cinder cones that typically occur on the flanks of volcanoes. Mohr and Wood (1976) have discovered a similar relationship between volcano spacing and alignment in Eastern Africa where widely scattered volcanoes occurring upon the Ethiopian Plateau are separated by greater distances, on the average, than volcanoes aligned along major rifts (for example, the Gregory Rift volcanoes).

FACTORS GOVERNING THE EMPLACEMENT OF CINDER CONE FIELDS

The morphometric measurements reported in this study indicate that platform cone fields are characterized by larger basal diameters and greater separation distances, on average, than cone fields formed on the flanks of volcanoes. Figure 4 shows that the average values of these two parameters vary in an approximately linear manner, such that

median cone diameter increases as median cone separation distance increases.

Fracture zones exposed upon the flanks of volcanoes commonly extend over a wide range of elevation, encompassing several kilometers of vertical topographic relief. There are numerous examples of eruptive activity moving to higher or lower elevations along such fracture zones during a particular eruption (1906 Vesuvius eruption, see Macdonald, 1972; 1959-1960 Kilauea eruption, see Richter and others, 1970; 1928 and 1971 Mt. Etna eruptions, see Macdonald, 1972, and Walker, 1973, respectively). The comparatively smaller average size and spacing of cinder cones formed upon the flanks of volcanoes may reflect the relative ease with which eruptive activity can shift to higher or lower elevations along a continuous fracture zone in response to variations in magmatic pressure during periods of active eruption. Such a mechanism would tend to limit the growth of individual cones and result in smaller separation distances between cones, as is observed within volcano cone fields.

In contrast, regional topographic variations across volcanic fields are typically much less than elevation differences encountered along the flanks of a volcano. Consequently, it is less likely that fluctuations in magmatic pressure would be compensated by the outbreak of eruptive activity at widely spaced locations, since local variations in surface overburden pressure are relatively small. In addition, the crustal basement underlying volcanic fields is typically crosscut by multiple sets of fractures rather than one or two major rift zones. Therefore, the mechanical force required to initiate an eruption at some new location is generally greater than the force required for magma to reach the surface via a rift zone

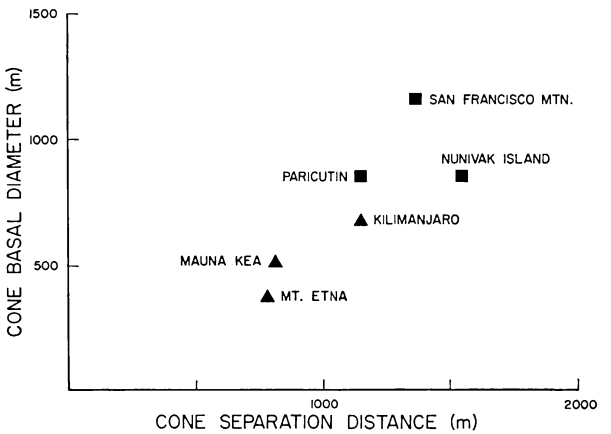

Fig. 4. Median values of cone basal diameter within individual cinder cone fields are plotted versus median values of cone separation distance in this graph (see table 2). Platform cone fields are represented by squares, and volcano cone fields are represented by triangles. The data trend indicates that average cone diameter and average cone spacing vary in an approximately linear manner.

fracture network. (Note that lateral confining pressures at shallow vertical depths are much greater within platform cone fields than within volcano cone fields.)

It is more probable that variations in magmatic pressure during volcanic field eruptions would be accommodated by changes in the rate at which pyroclastic material was discharged, rather than by wholesale shifts in the location of activity. This type of eruptive behavior was actually observed during the 1943-1944 Paricutin eruption in which explosive activity persisted at a single location over a period of ~12 months, while the pyroclastic production rate varied considerably (see Foshag and Gonzalez, 1956; note that this eruption may not be generally representative of all cone-forming eruptions). Lateral migration of explosive activity can occur on a local scale (on the order of 100-1000 m) within volcanic fields; variations in vent location on this scale lead to the construction of cinder cone clusters.

In summary, lateral shifts in exposive volcanic activity within volcanic fields may be generally inhibited due to relatively small regional variations in surface topography (that is, overburden pressures at depth) and the general absence of regional rift zones within this type of volcanic province. These circumstances would favor the construction of comparatively larger cinder cones separated by relatively greater distances, as is observed within platform cone fields.

IMPLICATIONS

1. McGetchin, Settle, and Chouet (1974) have conducted numerical simulations of cinder cone construction on other planetary surfaces employing measurements of eruption conditions obtained at North East Crater, Mt. Etna. Their results indicate that cinder cones on the Moon and Mars would generally possess smaller rim heights and larger basal diameters compared to terrestrial cones due to the reduced gravity and atmospheric drag encountered on these bodies. Calculated cone dimensions reported by McGetchin, Settle, and Chouet (1974) suggest that the basal diameter of lunar and martian cones would exceed the diameter of terrestrial cones by factors of 9 and 3½, respectively. On the Earth the average ratio of cone separation distance/cone basal diameter varies from 1.8 within volcano cone fields to 1.4 within platform cone fields (see table 2). Cinder cone spacing is largely controlled by the size and spacing of crustal fractures. Therefore, if terrestrial cone-forming eruptions were to occur on the Moon or Mars within an earth-like structural environment, cone basal diameter would be significantly greater than the diameter of terrestrial cones while the spacing between cones would be approximately the same. The models of McGetchin, Settle, and Chouet (1974) suggest that the ratio of cone separation distance/cone diameter would, on the average, be less than one within cone fields formed under these circumstances. This physically means that the exterior aprons of individual cones would generally overlap, and the pyroclastic material erupted from separate vents would merge to form a

hummocky, semi-continuous surface deposit. In this case a martian volcano cone field would consist of several, topographically subdued ridges of pyroclastic material radially aligned with respect to a volcano's summit; whereas a martian platform cone field would form a widespread mantling deposit.

2. Morphometric investigations of individual cone fields have suggested that variations in cinder cone shape can be correlated with the length of time a cone has been exposed to a particular set of erosive processes (Scott and Trask, 1971; Wood, 1979). This study has shown that the average ratio of cone height/diameter within a cone field is not directly correlated with the exposure age of the field. In particular, the average cone height/diameter ratio within the Nunivak Island and Mauna Kea cone fields was found to be significantly different, even though these two cone fields were constructed over contemporaneous periods of time. This implies that variations in weathering environment or eruption conditions may be equally as important as the age of a cone field in determining cone shape. Consequently, the relative ages of two or more cone fields *cannot* be inferred strictly on the basis of cone height/diameter relationships. Furthermore, it may be impossible to establish objective morphometric criteria for determining relative cone age within volcano cone fields, since cones constructed on the flanks of volcanoes are commonly exposed to a wide spectrum of degradation processes.

3. The volcanic activity responsible for the construction of a cinder cone field commonly represents the most recent phase of volcanism within a particular region (for example, Nunivak Island and San Francisco Mtn.). The distribution of the youngest cones within a field reflects the current configuration of subsurface conduits and dikes connecting the regional surface to magma storage reservoirs at depth. Cone fields in which volcanic activity has occurred during historical time may become prime candidate sites for geothermal energy production in the near future. In such cases, studies of cinder cone morphometry and distribution may be used to develop exploration strategies for conducting regional geophysical surveys prior to initiating exploratory drilling programs.

ACKNOWLEDGMENTS

Don Francis, Tom McGetchin, and Chuck Wood generously contributed a variety of maps to this project and freely shared ideas. The author is especially grateful for their assistance. This work was performed in part under NASA Grant NGR-40-002-116, which is appreciatively acknowledged. Special thanks to Jim Head, Fraser Goff, and Don Swanson for constructive reviews, and to Nancy Christy and Lisa Ranalli for their patience and diligence in preparing the manuscript. This paper constitutes Contribution 33 of the Basaltic Volcanism Study Project. The Project is organized and administered by the Lunar and Planetary Institute/Universities Space Research Association under contract NSR 09-051-001 with the National Aeronautics and Space Administration.

REFERENCES

Atwood, W. W., 1960, Red Mountain, Arizona: A dissected volcanic cone: Jour. Geology, v. 14, p. 138-146.

Bloomfield, K., 1975, A late-Quaternary monogenetic volcano field in central Mexico: Geol. Rundschau, v. 64, p. 476-497.

Carr, M. H., Greeley, R., Blasius, K. R., Guest, J. E., and Murray, J. B., 1977, Some martian volcanic features as viewed from the Viking Orbiter: Jour. Geophys. Research, v. 82, p. 3985-4015.

Colton, H. W., 1967, The basaltic cinder cones and lava flows of the San Francisco Mountain volcanic field, rev. ed.: Flagstaff, Ariz., Museum of Northern Arizona, 56 p.

Downie, C. and Wilkinson, P., 1972, The Geology of Kilimanjaro: Sheffield, England, University of Sheffield, Department of Geology, 250 p.

Eaton, J. P. and Murata, K. J., 1960, How volcanoes grow: Science, v. 132, p. 925-938.

Fiske, R. S. and Jackson, E. D., 1972, Orientation and growth of Hawaiian volcanic rifts: The effect of regional structure and gravitational stresses: Royal Soc. London Proc. A, v. 329, p. 299-326.

Foshag, W. F. and Gonzalez, J., 1956, Birth and development of Paricutin volcano, Mexico: U. S. Geol. Survey Bull. 965-D, p. 355-485.

Gutmann, J. T., 1976, Geology of Crater Elegante, Sonora, Mexico: Geol. Soc. America Bull., v. 87, p. 1718-1729.

Head, J. W., 1975, Morphology of pyroclastic lunar volcanic deposits: Implications for eruption conditions and localized sources of volatiles [abs.]: Houston, Texas, Lunar and Planetary Inst., Lunar Science VI, p. 349-351.

Hoare, J. M., Condon, W. H., Cox, A., Dalrymple, G. B., 1968, Geology, paleomagnetism, and potassium-argon ages of basalts from Nunivak Island, Alaska: Geol. Soc. America Mem. 116, p. 377-413.

Huntington, A. T., Walker, G. P. L., Argent, F. R. S., and Argent, C. R., 1974, United Kingdom Research on Mt. Etna: London, The Royal Soc., 74 p.

Kinoshita, W. T., 1965, A gravity survey of the island of Hawaii: Pacific Sci., v. 19, p. 341-342.

Macdonald, G. A., 1949, Petrography of the island of Hawaii: U.S. Geol. Survey Prof. Paper 214-D, 93 p.

———— 1972, Volcanoes: Englewood Cliffs, N.J., Prentice-Hall, Inc., 427 p.

Macdonald, G. A. and Katsura, T., 1964, Chemical compositions of Hawaiian lavas: Jour. Petrology, v. 5, p. 82-133.

McDougall, I., 1964, Potassium-argon ages from lavas of the Hawaiian Islands: Geol. Soc. America Bull., v. 75, p. 107-128.

Malahoff, A. and Woollard, G. P., 1966, Magnetic surveys over the Hawaiian Islands and their geologic implications: Pacific Sci., v. 20, p. 265-311.

McGetchin, T. R. and Head, J. W., 1973, Lunar cinder cones: Science, v. 180, p. 68-71.

McGetchin, T. R., Settle, Mark, and Chouet, B. A., 1974, Cinder cone growth modeled after Northeast Crater, Mt. Etna, Sicily: Jour. Geophys. Research, v. 79, p. 3257-3272.

Mohr, P. A., and Wood, C. A., 1976, Volcano spacings and lithospheric attenuation in the eastern rift of Africa: Earth Planetary Sci. Letters, v. 33, p. 126-144.

Moore, J. G., and Krivoy, H. L., 1964, The 1962 flank eruption of Kilauea volcano and structure of the east rift zone: Jour. Geophys. Research, v. 69, p. 2033-2045.

Moore, R. G., and Wolfe, E. W., 1976, Geologic map of the eastern San Francisco volcanic field, Arizona: U.S. Geol. Survey Misc. Inv. Series, Map I-953.

Moore, R. B., Wolfe, E. W., and Ulrich, G. E., 1976, Volcanic rocks of the eastern and northern parts of the San Francisco volcanic field, Arizona: U.S. Geol. Survey, Jour. Research, v. 4, p. 549-560.

Nakamura, K., 1977, Volcanoes as possible indicators of tectonic stress orientation—Principal and proposal: Jour. Volcan. Geotherm. Research, v. 2, p. 1-16.

Porter, S. C., 1972, Distribution, morphology, and size frequency of cinder cones on Mauna Kea Volcano, Hawaii: Geol. Soc. America Bull., v. 83, p. 3607-3612.

Porter, S. C., Stuiver, M., and Yang, I. C., 1977, Chronology of Hawaiian glaciations: Science, v. 195, p. 61-63.

Richter, D. H., Eaton, J. P., Murata, K. K., Ault, W. U., and Krivoy, H. L., 1970, Chronological narrative of the 1959-60 eruption of Kilauea Volcano, Hawaii: U.S. Geol. Survey Prof. Paper 537-E, 73 p.

Rittmann, A., 1963, Vulkanismus and tektonik des Atna: Geol. Rundschau, v. 53, p. 788-800.

———— 1973, Structure and evolution of Mount Etna: Royal Soc. London Philos. Trans. A., v. 274, p. 5-16.

Robinson, H. H., 1913, The San Franciscan volcanic field, Arizona: U.S. Geol. Survey Prof. Paper 76, 213 p.

Scott, D. H. and Trask, N. J., 1971, Geology of the Lunar Crater Volcanic Field, Nye County, Nevada: U.S. Geol. Survey Prof. Paper 599-I, 22 p.

Stearns, H. T. and Macdonald, G. A., 1946, Geology and groundwater resources of the island of Hawaii: Hawaii Div. Hydrography Bull. 9, 363 p.

Tanguy, J. C. and Kieffer, G., 1977, The 1974 eruption of Mt. Etna: Bull. volcanol., v. 40-4, p. 1-14.

Wadge, G., 1978, The storage and release of magma on Mt. Etna: Jour. Volcan. Geotherm. Research, v. 2, p. 361-384.

Walker, G. P. L., 1973, A brief account of the 1971 eruption of Mt. Etna: Royal Soc. London Philos. Trans. A., v. 274, p. 177-179.

Wernstedt, F. L., 1972, World Climatic Data: Lemont, Pa., Climatic Data Press, 522 p.

Williams, H., 1950, Volcanoes of the Paricutin region, Mexico: U.S. Geol. Survey Bull. 965-B, p. 165-274.

Wood, C. A., 1979, Morphometric evolution of cinder cones: Jour. volcanology geothermal Research, in press.